



Blocking the FKBP12 induced dendrimeric burst in aberrant aggregation of α -synuclein by using the ElteN378 synthetic inhibitor

Gabriella Caminati, Maria Raffaella Martina, Stefano Menichetti & Piero Procacci

To cite this article: Gabriella Caminati, Maria Raffaella Martina, Stefano Menichetti & Piero Procacci (2019) Blocking the FKBP12 induced dendrimeric burst in aberrant aggregation of α -synuclein by using the ElteN378 synthetic inhibitor, Journal of Enzyme Inhibition and Medicinal Chemistry, 34:1, 1711-1715

To link to this article: <https://doi.org/10.1080/14756366.2019.1667342>



© 2019 The Author(s). Published by Informa UK Limited, trading as Taylor & Francis Group.



View supplementary material [↗](#)



Published online: 24 Sep 2019.



Submit your article to this journal [↗](#)



View related articles [↗](#)



View Crossmark data [↗](#)

Blocking the FKBP12 induced dendrimeric burst in aberrant aggregation of α -synuclein by using the ElteN378 synthetic inhibitor

Gabriella Caminati^{a,b}, Maria Raffaella Martina^{a,b}, Stefano Menichetti^b and Piero Procacci^b

^aDepartment of Chemistry “Ugo Schiff”, University of Florence, Sesto Fiorentino, Italy; ^bCenter for Colloid and Surface Science (CSGI), University of Florence, Sesto Fiorentino, Italy

ABSTRACT

α -Synuclein (α -syn), a disordered cytoplasmatic protein, plays a fundamental role in the pathogenesis of Parkinson's disease (PD). Here, we have shown, using photophysical measurements, that addition of FKBP12 to α -syn solutions, dramatically accelerates protein aggregation, leading to an explosion of dendritic structures revealed by fluorescence and phase-contrast microscopy. We have further demonstrated that this aberrant α -syn aggregation can be blocked using a recently discovered non-immunosuppressive synthetic inhibitor of FKBP12, ElteN378. The role of FKBP12 and of ElteN378 in the α -syn aggregation mechanism has been elucidated using molecular dynamics simulations based on an effective coarse-grained model. The reported data not only reveal a new potent synthetic drug as a candidate for early stage treatment of α -syn dependent neurodegenerations but also pave the way to a deeper understanding of the mechanism of action of FKBP12 on α -syn oligomeric aggregation, a topic which is still controversial.

ARTICLE HISTORY

Received 3 July 2019
Revised 4 September 2019
Accepted 8 September 2019

KEYWORDS

FKBP12 inhibitor;
 α -synuclein; Parkinson's
disease; amyloid
aggregation; PD drug

Introduction

The plastic α -syn protein is a key player in the pathogenesis of Parkinson's disease (PD)^{1–3}. In pathological conditions, this protein is present in the brain cells in fibrillar, aggregated forms called Lewy bodies. Members of the FK506-binding protein (FKBP) family were recently shown to be implicated in neurological disorders and structure formation^{1,3,4}. The involvement of FKBP12 in the pathogenesis of α -syn-dependent neurodegeneration has been repeatedly shown in post-mortem studies on the brain of patients with neurodegenerative diseases^{1,5,6}. Recent investigations revealed an unbalance of the endogenous FKBP12 concentration in the very early stages of PD⁴, as well as the presence of FKBP12 in Lewy bodies⁶. Beeklandt and coworkers⁷ proposed that proteins of the FKBP family, and notably FKBP12, induce a faster aggregation of amyloid α -syn, by binding α -syn via the prolyl peptidyl isomerase domain⁸ to one of the proline in the hydrophilic C-terminus of the monomer⁹. Despite the cited mounting evidence about a possible role for FKBP12 in synucleopathies and neurological disorders through the enhancement of α -syn aggregation, the mechanism of such enhancement has not been unraveled yet.


In Figure 1, we show a ribbon representation of α -syn monomer along with the FKBP12 protein. The α -syn monomer primary structure comprises three distinct segments. The C terminus (92–140) is a polar coil region bearing a strong negative charge (–15e) and hosting all five prolines in α -syn. The equally polar 1–40 N α -helical¹⁰ terminus has a mixture of negatively and positively charged residues with a slight prevalence of the latter (+3e). The central NAC domain, including amino-acids 40 to 92, is

characterised by a sequence of mostly hydrophobic residues and is involved in β -sheet formation¹¹. Several studies have shown that α -syn fibrils are characterised by a β -rich hydrophobic solvent protected core^{12–15} with external hydrophilic filaments due to the C and N termini.

Using a combined approach of experimental measurements and molecular dynamics simulations, in this contribution we aim at elucidating the role of FKBP12 in α -syn aggregation kinetics and aggregate morphology suggesting at the same time a possible therapeutic agent, the synthetic ElteN378 FKBP12 inhibitor¹⁶, in PD neuropathies. ElteN378 is a low atomic weight FKBP12 ligand with affinity comparable to that of the natural binder FK506. This ligand is affordable from commercially available precursors and, as shown in Supplementary Figure S1 in Supporting Information, has been designed to optimally expose the two contiguous carbonyl oxygen atoms in the proline-mimetic chain for H-bond-driven FKBP12 docking¹⁶.

Aggregation of α -syn was studied *in vitro* following the change in the photophysical behaviour of the fluorescent probe ThT in three different systems: α -syn, α -syn/FKBP12 1:1 and α -syn/FKBP12 1:1 inhibited by ElteN378. Imaging of mature aggregates of the previous systems was obtained with fluorescence and phase-contrast microscopy. The collected experimental evidence on aggregation kinetics and morphology was interpreted using extensive MD simulations based on a coarse-grained model (CG) for α -syn and α -syn-bound FKBP12 monomers with inter- and intra-molecular interactions driven by a potential mean force effectively accounting for the amphiphilic nature of the α -syn monomer. The results showed striking similarities between the

CONTACT Piero Procacci ✉ piero.procacci@unifi.it; Gabriella Caminati ✉ gabriella.caminati@unifi.it Department of Chemistry “Ugo Schiff”/CSGI, University of Florence, Via della Lastruccia 3-13, Sesto Fiorentino, I-50019 Italy

 Supplemental data for this article can be accessed [here](#).

© 2019 The Author(s). Published by Informa UK Limited, trading as Taylor & Francis Group.

This is an Open Access article distributed under the terms of the Creative Commons Attribution License (<http://creativecommons.org/licenses/by/4.0/>), which permits unrestricted use, distribution, and reproduction in any medium, provided the original work is properly cited.

structures obtained from the CG simulations and the experimentally observed morphology of the aggregates suggesting that the mechanism and fate of the aggregation process can be dramatically modified by altering the balance between hydrophilic and hydrophobic forces.

Aggregation kinetics

Unseeded samples were incubated at 37 °C in glass vials under gentle constant stirring¹⁷. We used 1 μ M concentration for both α -syn and FKBP12 in Tris buffer. The physiological cytosolic concentration of α -syn in brain cells was reported to be¹⁸ in the low micromolar range and is probably even below this level¹⁹. On the other hand, FKBP12 is especially abundant in brain²⁰ with physiological concentrations reaching 3 μ M, according to recent studies²¹.

Aliquots of the incubated solutions were withdrawn and characterised at different time intervals for 20 weeks. ThT was added only before each measurement to avoid probe-induced artifacts on aggregation. At the working ThT concentration used in this work (3 μ M), the probe is present in solution exclusively as monomer and the corresponding emission spectrum shows a single weak emission band centred at 445 nm (Supplementary Figure S4a) upon excitation at 350 nm, as commonly found^{22,23} for ThT monomer in protic solvents. Control experiments exclude ThT interaction with native α -syn or with the globular FKBP12, in agreement with literature reports²⁴. Further details on the experimental procedures are reported in Supporting Information.

When ThT was added to α -syn solutions we observed a significant change in the position and the intensity of the excitation and emission bands: in Figure 2, we report the ThT fluorescence intensity at $\lambda_{em} = 480$ nm with $\lambda_{exc} = 410$ nm as a function of time for all examined systems. For free α -syn, in the absence of any added seed, ThT emission intensity changes with time following the well-known sigmoidal curve^{23,25} although the lag phase is contracted in this time scale. The curve is consistent with a nucleation-dependent elongation model of fibril formation^{26,27}. After 18 days, aggregation proceeds through elongation of the protofibrils without further change in ThT emission. In the equimolar α -syn-FKBP12 system, fluorescence emission increases at a faster rate reaching larger intensity values at a much earlier stage (10 days), before decreasing to a plateau value.

Addition of 200 nM ElteN378 inhibitor in the FKBP12- α -syn system results in a similar kinetic profile but with a reduction of the aggregated phase, followed, once more, by a decrease in ThT signal. While rarely reported in conventional aggregation studies²⁸, the decrease in ThT fluorescence in aged α -syn containing solutions, consistently detected in all analysed independent samples can be explained by a combination of chemical-physical effects that include (i) redistribution of the ThT probe in other sites of the growing oligomers characterised by a shift of the maximum of ThT emission band, (ii) formation of mature aggregates with different morphology and exposed β -sheet content (interconverting structures), and (iii) partial loss of emission intensity due to deposition of fibrillar tangles. The stabilisation of the ThT fluorescence signal in long term measurements allows for the exclusion of progressive sedimentation of large aggregates.

In order to elucidate the observed aggregation kinetics, we have done extensive MD simulations based on an elementary CG model for α -syn and α -syn-bound FKBP12 using the program ORAC^{29,30}. Computational details on the CG approach are provided in Supporting Information. Briefly, we adopt a 15 beads CG representation of the monomeric α -syn chain, made up of three

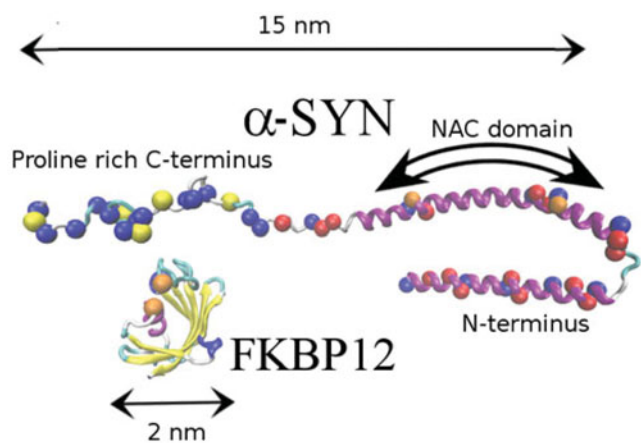


Figure 1. α -syn and FKBP12 structures. Red and blue balls on α -SYN indicate negatively and positively charged residues, respectively. Proline is indicated in yellow colour.

distinct parts of five beads length each: a central hydrophobic part representing the NAC domain and two terminal hydrophilic parts. The five beads approach is based on a recent model for the α -syn mature fibrils based on a five strands monomer^{11,31,32}. We use a solvent-free model with renormalised bead-bead non-bonded interactions so as to mimic, in a water environment, the aggregation of hydrophobic moieties and solubilisation of the hydrophilic groups. We further assume that, when proline-bound to the C terminus of α -syn, the globular protein FKBP12 exposes an unsaturated β -strand acting as a seed for the binding of the β -sheet forming NAC domain, as illustrated in Figure 1.

The FKBP12 addition at the onset of α -syn aggregation is hence modelled by simply replacing one of the terminal hydrophilic beads with a hydrophobic one in a fraction, say ϕ , of α -syn monomers computed according to the nominal concentration of the species and to the equilibrium dissociation constant for the FKBP12- α -syn complex estimated to be in the micromolar range (see Supporting Information). The effect of the tight-binding ElteN378 inhibitor in the α -syn-FKBP12 solution is simply that of reducing the FKBP12-effective concentration in a strictly dose-dependent manner. In Figure 3, we show the calculated CG kinetics for the pure α -syn and for samples with different fractions ϕ of FKBP12-modified α -syn monomers. Inspection of Figure 3 shows that the kinetics is accelerated with increasing fraction of FKBP12-modified α -syn molecules. Correspondingly, the final stationary value of the average number n_{mol} grows with the fraction of FKBP12-bound α -syn monomers, ending up to only few supra-molecular macro-aggregates for $\phi > 0.5$. In the inset, we report the final value of n_{mol} as a function of ϕ evidencing the non-linear effect of FKBP12 addition. Up to $\phi = 0.3$, the aggregation kinetics resembles that observed in the sample of pure α -syn. Above the threshold fraction of $\phi > 0.3$, the aggregation kinetics undergoes an abrupt regime cross-over, exhibiting a much faster growth

Aggregation morphology

Aliquots of the mature incubated solutions were imaged by means of fluorescence and phase-contrast microscopy. Typical fluorescence images, consistently observed in all independent samples, are reported in Figure 4 while typical phase contrast results are shown in Supplementary Figure S2. As shown in the upper panel left image of Figure 4, images of α -syn at very long aggregation times show the presence of a high concentration of linear structures as found also by other authors¹⁴.

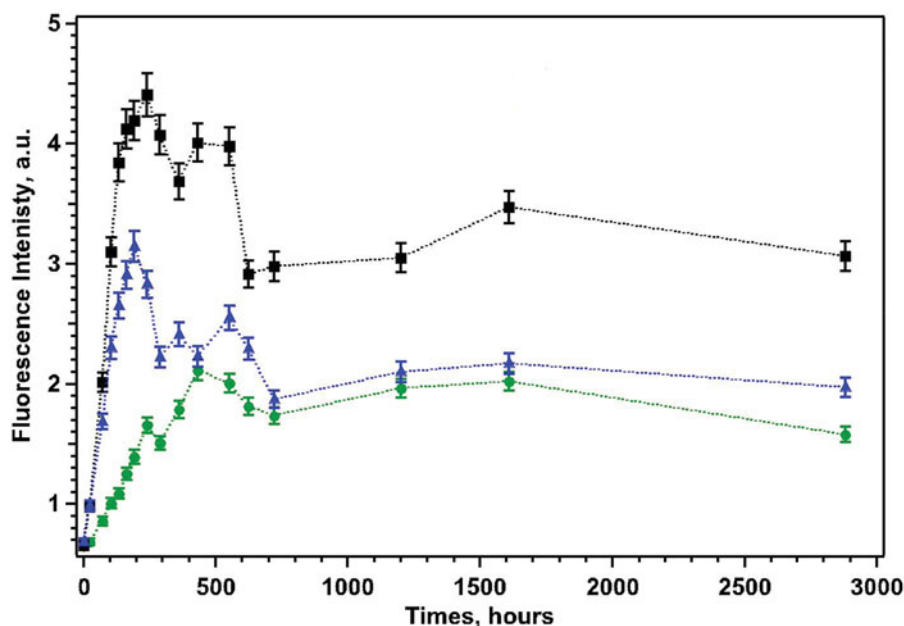


Figure 2. Fluorescence emission intensity at $\lambda = 480$ nm for α -syn (green circles), α -syn/FKBP12 (black squares) and α -syn/FKBP12/ElteN378 (blue triangles) systems. For each system, the reported error bars have been computed by analysing the ThT fluorescence intensity measured in three independent samples (see Supporting Information for further details).

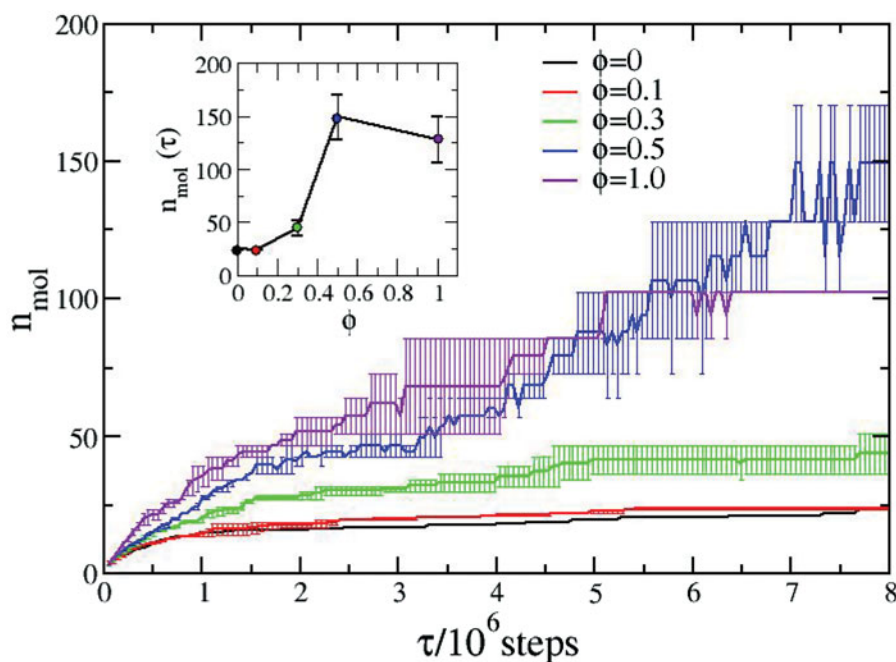


Figure 3. Aggregation kinetics measured by the average number of monomers composing the aggregates for various fractions ϕ (see text) of FKBP12-bound α -syn. The total number of the 15-beads α -syn monomers is in all case equal to 512. For each fraction, the errors have been evaluated by averaging the data over three independent simulations. In the inset, we report the average number of monomers composing the aggregates in the final configuration.

The linear morphology of the fibril in α -syn aggregation has been rationalised^{32,33} in terms of an in-register parallel β -sheet structure with systematic stacking of the hydrophobic NAC domains of the monomers along the fibril axis. The central upper panel of Figure 4 shows images of samples taken from an equimolar solution of FKBP12- α -syn. The observed aggregation pattern is dramatically different, exhibiting an impressive dendritic explosion of highly branched structures. Remarkably, such quasi-fractal growth is strongly reduced when ElteN378 is present in the α -syn/FKBP12 system: the number of branching nodes is drastically scaled down resulting in much smaller and less abundant

aggregates with a cross-like morphology. The rationale for the observed behaviour lies in the strong binding affinity of ElteN378 for FKBP12, previously reported by us¹⁶. The presence of the tightly bound ElteN378 in the FKBP12 substrate pocket prevents the possibility of FKBP12 to interact with the proline-rich C terminus of α -syn. This translates in a reduction of the concentration of "active" FKBP12 seeds for explosive branching of α -syn aggregates.

The lower panel of Figure 4 refers to the end states of the CG simulations for different fraction of FKBP12-doped α -syn. In striking correspondence with the experimental observations, the

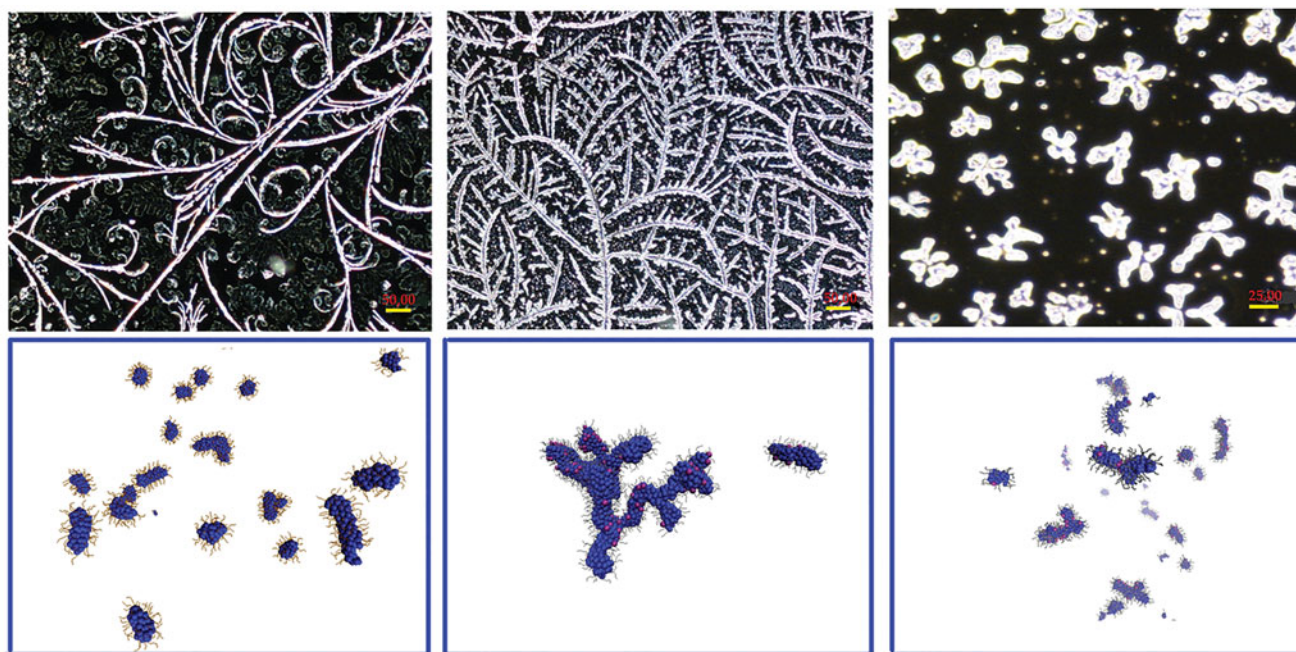


Figure 4. Upper panel: fluorescence images of mature fibrillar aggregates. Left: aggregated pure α -syn. Central: dendritic aggregated structures for equimolar mixtures of FKBP12/ α -syn. Right: small cross-like or star-like amorphous structures of the three components system: ElteN378/FKBP12/ α -syn. Lower panel snapshots of three MD simulations based on a CG model: α -syn alone (left), α -syn/FKBP12 mixture (central) and ElteN378/FKBP12/ α -syn mixture (right). Hydrophobic beads are shown as blue spheres. FKBP12-bound beads are shown as red spheres. Hydrophilic N- and C-terminus beads are shown in orange bond representation.

sample containing only α -syn ($\phi=0$) spontaneously aggregates in linear fibrils exposing the hydrophilic filaments towards the solvent, roughly perpendicularly to the fibril axis. When one-third of the α -syn monomers are FKBP12-doped ($\phi=0.3$), the final supramolecular aggregates are poorly branched (right lower panel). The same morphology is observed experimentally in the ElteN378-FKBP12 α -syn mixture. As above outlined, when $\phi>0.3$, the kinetics undergoes a drastic change, with the sample ending up in forming few highly branched macro-aggregates (central lower panel). In Supporting Information, we estimate that in the equimolar FKBP12- α -syn solution the fraction α -syn monomers bearing a bound FKBP12 is in the range $\phi=0.3:0.4$. The estimate is based on the measure of the fluorescence quenching of the strong tryptophan emission band at 300–350 nm occurring in FKBP12 solutions upon ligand addition. The presence of the tight-binding inhibitor ElteN378 in FKBP12- α -syn mixture lowers this fraction below 0.3, corresponding to the value for the cross-over regime reported in the inset of Figure 3).

Conclusions

We have shown using ThT fluorescence and microscopy, that FKBP12 and α -syn in a 1:1 molar ratio spontaneously aggregate forming a dendritic explosion of aggregated structures. This process can be tamed, in a dose-dependent manner, using the non-immunosuppressive ElteN378 synthetic inhibitor. CG simulations showed that the aggregation of α -syn in linear fibrils as well as in complex branched supramolecular aggregates is elicited by the hydrophobic aggregation of the central non-polar NAC residues of the monomeric unit. Remarkably, our rudimentary CG model for the α -syn monomer was able to reproduce the essential morphological features of the supramolecular aggregates in the final stages with no necessity of introducing any detail on the secondary structure, therefore hinting that a continuous and variegated β -reorganisation process follows the primary event of hydrophobic-driven association of the NAC domains in oligomers.

Acknowledgements

We thank MIUR-Italy (“Progetto Dipartimenti di Eccellenza 2018-2022” allocated to Department of Chemistry “Ugo Schiff”).

Disclosure statement

No potential conflict of interest was reported by the authors.

References

1. Avramut M, Achim C. Immunophilins and their ligands: insights into survival and growth of human neurons. *Physiol Behav* 2002;77:463–8.
2. Shults CW. Lewy bodies. *Proc Natl Acad Sci USA* 2006;103:1661–8.
3. Gerard M, Deleersnijder A, Daniels V, et al. Inhibition of FK506 binding proteins reduces α -synuclein aggregation and Parkinson’s disease-like pathology. *J Neurosci* 2010;30:2454–63.
4. Nilsson A, Sköld K, Sjögren B, et al. Increased striatal mRNA and protein levels of the immunophilin FKBP-12 in experimental Parkinson’s disease and identification of FKBP-12-binding proteins. *J Proteome Res* 2007;6:3952–61.
5. Sugata H, Matsuo K, Nakagawa T, et al. A peptidyl-prolyl isomerase, FKBP12, accumulates in Alzheimer neurofibrillary tangles. *Neurosci Lett* 2009;459:96–9.
6. Honjo Y, Ayaki T, Horibe T, et al. FKBP12-immunopositive inclusions in patients with α -synucleinopathies. *Brain Res* 2018;1680:39–45.
7. Deleersnijder A, Van Rompuy AS, Desender L, et al. Comparative analysis of different peptidyl-prolyl isomerases reveals FK506-binding protein 12 as the most potent

- enhancer of α -synuclein aggregation. *J Biol Chem* 2011;286:26687–701.
8. Gerard M, Debyser Z, Desender L, et al. FK506 binding protein 12 differentially accelerates fibril formation of wild type alpha-synuclein and its clinical mutants A30P or A53T. *J Neurochem* 2008;106:121–33.
 9. Meuvius J, Gerard M, Desender L, et al. The conformation and the aggregation kinetics of α -synuclein depend on the pro-line residues in its C-terminal region. *Biochemistry* 2010;49:9345–52.
 10. Haney CM, Petersson EJ. Fluorescence spectroscopy reveals N-terminal order in fibrillar forms of α -synuclein. *Chem Commun* 2018;54:833–6.
 11. Vilar M, Chou HT, Lührs T, et al. The fold of alpha-synuclein fibrils. *Proc Natl Acad Sci USA* 2008;105:8637–42.
 12. Chen M, Margittai M, Chen J, Langen R. Investigation of alpha-synuclein fibril structure by site-directed spin labeling. *J Biol Chem* 2007;282:24970–9.
 13. Cho MK, Kim HY, Fernandez CO, et al. Conserved core of amyloid fibrils of wild type and A30P mutant α -synuclein. *Protein Sci* 2011;20:387–95.
 14. Sweers KKM, van der Werf KO, Bennink ML, Subramaniam V. Atomic force microscopy under controlled conditions reveals structure of C-terminal region of α -synuclein in amyloid fibrils. *ACS Nano* 2012;6:5952–60.
 15. Xu L, Bhattacharya S, Thompson D. Re-designing the α -synuclein tetramer. *Chem Commun* 2018;54:8080–3.
 16. Martina MR, Tenori E, Bizzarri M, et al. The precise chemical-physical nature of the pharmacore in FK506 binding protein inhibition: ElteX, a new class of nanomolar FKB12 ligands. *J Med Chem* 2013;56:1041–51.
 17. Brown JWP, Meisl G, Knowles TPJ, Buell AK, et al. Kinetic barriers to α -synuclein protofilament formation and conversion into mature fibrils. *Chem Commun* 2018;54:7854–7.
 18. Iwai A, Masliah E, Yoshimoto M, et al. The precursor protein of non-A β component of Alzheimer's disease amyloid is a presynaptic protein of the central nervous system. *Neuron* 1995;14:467–75.
 19. Iljina M, Garcia GA, Horrocks MH, et al. Kinetic model of the aggregation of alpha-synuclein provides insights into prion-like spreading. *Proc Natl Acad Sci USA* 2016;113:E1206–E1215.
 20. Lyons W, Steiner JP, Snyder SH, Dawson TM. Neuronal regeneration enhances the expression of the immunophilin FKBP-12. *J Neurosci* 1995;15:2985–94.
 21. Galfré E, Pitt SJ, Venturi E, et al. FKBP12 activates the cardiac ryanodine receptor Ca^{2+} -release channel and is antagonised by FKBP12.6. *PLoS One* 2012;7:e31956–16.
 22. Amdursky N, Erez Y, Huppert D. Molecular rotors: what lies behind the high sensitivity of the Thioflavin-T fluorescent marker. *Acc Chem Res* 2012;45:1548–57.
 23. Biancalana M, Koide S. Molecular mechanism of Thioflavin-T binding to amyloid fibrils. *Biochim Biophys Acta* 2010;1804:1405–12.
 24. Ghosh D, Singh PK, Sahay S, et al. Structure based aggregation studies reveal the presence of helix-rich intermediate during α -Synuclein aggregation. *Sci Rep* 2015;5:9228.
 25. Sulatskaya AI, Maskevich AA, Kuznetsova IM, et al. Fluorescence quantum yield of Thioflavin T in rigid isotropic solution and incorporated into the amyloid fibrils. *PLoS One* 2010;5:e15385–7.
 26. Wood J, Wypych J, Steavenson S, et al. α -Synuclein fibrillogenesis is nucleation-dependent: implications for the pathogenesis of Parkinson's disease. *J Biol Chem* 1999;274:19509–12.
 27. Bharathi P, Nagabhushan P, Rao K. Mathematical approach to understand the kinetics of α -synuclein aggregation: relevance to Parkinson's disease. *Comput Biol Med* 2008;38:1084–93.
 28. Lindberg DJ, Wranne MS, Gatty MG, et al. Steady state and time-resolved Thioflavin-T fluorescence can report on morphological differences in amyloid fibrils formed by A β (1-40) and A β (1-42). *Biochem Biophys Res Commun* 2015;458:418–23.
 29. Procacci P. Hybrid MPI/OpenMP implementation of the ORAC molecular dynamics program for generalized ensemble and fast switching alchemical simulations. *J Chem Inf Model* 2016;56:1117–21.
 30. Procacci P. Orac 6. 2017. Available from: <http://www.chim.unifi.it/orac>. [last accessed 13 Sep 2019].
 31. Esteban-Martín S, Silvestre-Ryan J, Bertoncini CW, Salvatella X. Identification of fibril-like tertiary contacts in soluble monomeric α -synuclein. *Biophys J* 2013;105:1192–8.
 32. Hashemi Shabestari M, Kumar P, Segers-Nolten I, et al. Three long-range distance constraints and an approach towards a model for the α -synuclein-fibril fold. *Appl Magn Reson* 2015;46:369–20.
 33. Sweers KKM, Segers-Nolten IMJ, Bennink ML, Subramaniam V. Structural model for alpha-synuclein fibrils derived from high resolution imaging and nanomechanical studies using atomic force microscopy. *Soft Matter* 2012;8:7215–22.